Influence of the nature and amount of carbonate additions on the thermal behaviour of geopolymers: A model for prediction of shrinkage

Svetlana Petlitckaia, Ameni Gharzouni, Eloise Hyvernaud, Nathalie Texier-Mandoki, Xavier Bourbon, Sylvie Rossignol

Influence of the nature and amount of carbonate additions on the thermal behaviour of geopolymers: A model for prediction of shrinkage

Svetlana Petlitckaia[1], Ameni Gharzouni[1], Eloise Hyvernaud[1], Nathalie Texier-Mandoki[2], Xavier Bourbon[2], Sylvie Rossignol[1]

[1]Institut de Recherche sur les Céramiques (IRCER), 12 rue Atlantis, 87068 Limoges Cedex, France

[2]Agence nationale pour la gestion des déchets radioactifs, 1-7 rue Jean-Monnet, 92298 Châtenay-Malabry Cedex, France

Abstract:

In order to develop fire resistant geopolymer materials, it is necessary to understand the parameters controlling their thermal behavior such as the content of alkali or rare earth cations. This study highlights the effect of carbonate nature and amount on the thermal behavior of geopolymers in order to propose a model of thermal behaviour and predict shrinkage. For this, various mixtures of kaolin and calcite and/or dolomite with different percentages were calcined at 600 and 750°C. The feasibility of consolidated materials based on these mixtures were evaluated and the thermal behavior of the obtained materials was investigated. The characterization of the mixtures revealed the persistence of carbonates after calcination at 600°C and their partial decomposition after calcination at 750°C. This fact was explained in the case of high dolomite content by the existence of kaolinite gangue hindering its decomposition. Consolidated materials were obtained from the different mixtures. After thermal treatment at 1000°C, it was evidenced that the amorphous phase crystallizes to form in a major part leucite. At lower available alkaline earth species (Ca^{2+} and Mg^{2+}) content, only wollastonite is formed and the shrinkage varies between 15 and 12%. However, at higher content, different calcium and magnesium silicates can be formed such calico-olivine and larnite in the case of calcite based materials and akermanite and merwinite for dolomite based

materials. This fact leads to lower shrinkage value (from 6 to 8%). Thus, it is possible to control the thermal behavior and predict the shrinkage of geopolymer materials by controlling the available alkaline earth cations.

Keywords: kaolin; calcite; geopolymer; dolomite; shrinkage

1. Introduction

Geopolymers are amorphous three-dimensional aluminosilicate material resulting from the condensation of alumina and silica sources at high pH and low temperature (less than 100 °C) [1]. They are characterized by high mechanical properties, stability at high temperatures [2], wide range of applications [3] and low environmental impact [4]. Calcined clays are often used as aluminosilicate source for geopolymer synthesis [5,6]. They are generally composed of clays minerals, tectosilicates and carbonates. The understanding of the structural evolution of each component of the clays and the interactions between them upon thermal treatment is crucial to determine their reactivity and their effect on the geopolymer properties such as thermal resistance. Carbonate is one of the most abundant and reactive compounds on earth. Their thermal decomposition was intensively studied because of its great technological importance [7]. Different parameters can influence the carbonate thermal decomposition such as the nature and crystalline structure of carbonate and the experimental conditions such as the sample weight, the particle size, the purge gas… [8]. Calcite is the most stable crystalline form of calcium carbonate. It was proven to decompose at 750°C [9]. Dolomite was shown to decompose in two stages. The first one yield to the formation of MgO and CaO. Then, the CaO reacts to form calcite if sufficient CO_2 is available [10]. The interaction between kaolinite and calcite upon thermal treatment was also studied [11, 12]. It was evidenced that calcite endothermic peak on differential thermal analysis curve was impacted by the ratio of kaolinite to calcite, the rate of CO_2 flow, the mixing, the heating rate and the volatiles evolved during the dehydroxylation of kaolinite. Mitchell et al., [13] have proven that the heat

treatment of a mixture of 95% of kaolinite and 5% of calcite leads to the dehydroxylation of kaolinite at 600°C, the decomposition of calcite to form lime (CaO) and portlandite ($Ca(OH)_2$) if high humidity. From 900°C, it was evidenced the formation of anorthite ($CaAl_2Si_2O_8$) and gehlenite ($Ca_2Al(Al\ Si)O_7$) and a beginning of formation of mullite ($Al_6Si_2O_{13}$) due to the excess of metakaolinite. Mixtures of kaolin and dolomite were also studied with the same proportions. Dolomite decomposed between 500 and 600 °C to form lime and periclase. At 900 °C, there is formation of gehlenite and anorthite, and persistence of periclase (MgO). Other studies investigated kaolin and dolomite mixture to produce macroporous support for ceramic membranes [14]. They have demonstrated that the sintering of kaolin was inhibited by a percentage of dolomite higher than 10 wt. %. The crystalline phases formed by in situ reaction sintering between 1150 and 1300 °C were mullite, cordierite ($Al_3Mg_2AlSi_5O_{18}$) and anorthite.

Several studies [15,16,17,18] have focused on the effect of carbonates on geopolymer synthesis and properties. Kutuk and Cetinkaya [19] have shown that kaolinite-calcite based geopolymer materials can be successfully synthesized with various mass ratios of kaolinite and using alkali silicate and NaOH. Yip et al., [20] have demonstrated that the addition of 20 wt.% of calcite and dolomite to metakaolin has a beneficial effect on the mechanical properties of geopolymers. Above this percentage, the formation of geopolymer is limited and the shrinkage is increased. Valentini et al., [21] also demonstrated that the moderate addition of calcium carbonate (~ 25 wt. %) induces a significant increase of compressive strength. However, the mechanical strength of geopolymer based on dolomite-metakaolin were found to be lower than the calcite based one [22] due to lower dissolved calcium, particle size and surface properties differences of dolomite compared to calcite. Although the effect of carbonates on the mechanical properties was understood, their effect on the thermal behavior is still complex and obvious as it depends on their amount and structure [23]. Dupuy et al.,

[24,25] have studied the thermal behavior of argillite based alkali-activated materials. The studies evidenced that carbonates, essentially calcite and a low amount of dolomite, initially present in the argillite, decompose during thermal treatment. Thus, available calcium reacts with silica from the geopolymer amorphous phase to form wollastonite. Few studies investigate the thermal evolution of geopolymers based on dolomite. Yan et al.,[26] evidenced that the thermal treatment at 1000 °C of geopolymer foams based on metakaolin and dolomite leads to the crystallization of leucite and the formation of periclase and lime resulting from the decomposition of dolomite. Consequently, the presence of carbonates depending on their nature and amount leads at high temperature of the formation of crystalline phases due to solid state reaction. In previous work [27], it was demonstrated that geopolymers based on a mixture of 33 wt. % of kaolin and 67 wt. % of argillite calcined at 750°C exhibit a high thermal treatment resistance at 1000°C with an improvement of post-thermal treatment strength. In order to understand this behavior and to propose a model of reactivity of this sample, different mixtures based on kaolin and carbonates (calcite and/or dolomite) with different proportions and calcination temperature (600 and 700°C) are investigated in the present study. Thus, the novelty of the study is to give further insight on the thermal behavior of geopolymer by understanding the role played by carbonate type and amount as well as the calcination temperature of the aluminosilicate source and to propose a model of thermal behaviour. In the discussion part, other formulations were added in order to validate the obtained results.

2. Experimental part

2.1. Raw materials and sample preparation

The starting materials are reported in Table 1. The kaolin (Si/Al =1.44) contains traces of calcite [28]. The mean diameter of kaolin is 20 µm and its water demand is about 530 µL/g. The BET specific surface area is 24 m^2/g. The calcite ($CaCO_3$) and dolomite

($CaMg(CO_3)_2$) have close water demand (310 and 273 µL/g respectively) with the different particles size (2 and 14 µm respectively). $CaCO_3$ and $CaMg(CO_3)_2$ have both similar specific surface areas (2 and 1 m^2/g respectively). A commercial potassium silicate solution (Woellner GmbH, Gemany), with Si/K molar ratio of 1.7 and 79 % of water content, was used. The activation solution, labelled S, was prepared by dissolving potassium hydroxide pellets in this commercial solution in order to obtain a Si/K molar ratio of 0.58.

Five mixtures were prepared as shown in the $CaO\text{-}MgO\text{-}2SiO_2Al_2O_3$ ternary diagram (**Figure 1**): (i) Two mixtures containing kaolin and calcite with weight percentages of calcite equal to 10 and 50 wt. %, which corresponds to 21 and 70 molar percentages respectively (ii) Two mixtures containing kaolin and dolomite with weight percentages of dolomite of 10 and 50 wt. % which corresponds to molar percentages of dolomite of 13 and 57 % and (iii) a mixture containing kaolin (82 wt. %), calcite (13 wt. %) and dolomite (5 wt. %) corresponding to molar percentages of 70, 25 and 5 %, respectively. The homogenization of the mixtures was performed using a turbula mixer for 1 hour with a rotation speed of 72 rpm. Then, the mixtures were calcined at 600 and 750 °C in a rotary oven (Carbolite Gero) for 1.5 hours except of the mixture containing calcite and dolomite which was only calcined at 750°C in order to model the sample studied in previous work and showing optimal thermal resistance at 1000°C [26]. The geopolymer samples are prepared by mixing the calcined mixtures with the activation solution for 5 min. The K_2O/H_2O molar ratio is about 18.7. The samples are cast in closed polysterene mold (Ø =25 mm, H = 60 mm) and kept at room temperature for 7 days. Then, the thermal resistance of the different samples was evaluated at 1000°C with a ramp of 5°/min, a dwell time of 15 min and a natural cooling in the furnace.

The adopted nomenclature to identify the raw mixtures and the geopolymer samples is M_x^T and GM_x^T respectively, with M= ca and/or do, “ca” refers to calcite, “do” to dolomite and “x to the weight percentage of each component. “T” indicates the calcination temperature (T=

600 or 750 °C). For example, $Gca_{0.1}^{600}$ geopolymer sample was obtained by mixing the silicate solution with the mixture $ca_{0.1}^{600}$ composed of 90 wt.% of kaolin and 10 wt.% of calcite calcined at 600 °C.

2.2. Characterization techniques

The particle size distributions of the raw materials and the mixtures were measured using a laser particle size analyzer (Mastersizer-2000). The powders were dispersed in water.

Powder BET areas (m^2/g) were determined by N_2 adsorption at -195.85 °C using a Micrometrics Tristar II 3020 volumetric adsorption/desorption apparatus. Prior to the measurement, the samples were degassed at 200 °C under vacuum for 4h.

The water demand (µL/g) corresponds to the volume of water that can adsorbed by one gram of powder before saturation. One gram of powder is deposited on a glass slide; water is then added to the powder using a micropipette until visual saturation.

Differential thermal analysis (DTA) and thermogravimetric analysis (TGA) were performed with a TA Instrument SDT Q600. Measurements were carried out under dry airflow (100 mL/min) in a platinum crucible. About 30 mg of crushed samples were heated up to 1000 °C with a rate of 10 °C/min and a dwelling time of 15 min. DTA-TGA coupled with mass spectrometry was performed with a Netzsch STA 449F3 analyzer. For these measurements, the samples were heated to 900 °C at a rate of 10 °C/min under an argon flow.

Fourier-Transform Infrared (FTIR) spectra were obtained with a ThermoFisher Scientific Nicolet 380 spectrometer on the raw and calcined mixtures. Spectra were acquired in transmission mode using KBr pressed discs (100 mg of KBr and 0.6 mg of sample). The spectra were recording between 400 and 4000 cm^{-1} with a 4 cm^{-1} resolution and composed of 64 scans. The atmospheric CO_2 contribution was removed by using a straight line between 2400 and 2280 cm^{-1}. To allow comparison between the spectra, they were corrected using a baseline and were normalized.

X-ray diffraction (XRD) experiments were performed with a Brucker-D8 Advance which operates with Bragg-Brentano geometry and a CuK$\alpha_1\alpha_2$ detector. Data were recorded at a range of 10°- 50 ° (2θ) with an angular step size of 0.02 °(2θ) and a counting time of 0.26 s per step. Joint Committee Powder Diffraction Standard (JCPDS) files were used for phase identification.

Dilatometric measurements were performed under air with a vertical dilatometer Setsys made by Setaram Instrumentation. The cylindrical samples (d/ H = 0.6, where d= 5 mm and H = 8 mm) were placed between two platinum/alumina holders during the analysis, and a correction was applied to remove the contribution of the device/ holders. Samples were heated until 900°C with a ramp of 5°C /min in an air atmosphere and cooled with a ramp of 20 °C/min

Environmental Scanning Electron Microscopy experiments were conducted using a FEI QUANTA 450 FEG microscope at 15 kV. The geopolymer sample was directly placed in a small MgO crucible covered with platinum paint (5 mm inner diameter). The thermocouple is placed below the sample. The temperature was increased from 25 to 1000°C. The pressure is maintained at 200 Pa. Many images of the sample surface were recorded during the temperature variation.

III. Results and discussion

1) Effect of carbonate nature and amount and the temperature of thermal treatment on kaolin-carbonates mixtures

In order to understand the thermal evolution of kaolin-carbonates mixtures, they were characterized using thermal analysis, FTIR spectroscopy, XRD, chemical and physical characterization. The effect of carbonate nature and amount and the temperature of thermal treatment was highlighted.

a) Structural characterization

FTIR measurements were also performed on the different mixtures. **Figure 4** shows the FTIR spectra of the different mixtures. Whatever the non-calcined mixture (**Figure 4 A),** bands related to OH stretching vibrations at 3396, 3650 and 3620 cm^{-1} and bending vibration at 913 (Al_2OH) cm^{-1} [29] are observed. These bands are characteristic of kaolinite [30]. The Si–O stretching vibrations are observed at 1100, 1034 and 1007 cm^{-1} [32]. The doublet at 797 and 778 cm^{-1} and the peak at 694 cm^{-1} are attributed to quartz [31]. For kaolin-calcite mixtures, in addition to bands relative to kaolinite, asymmetric stretching vibrations (υ_3) at 1430 cm^{-1} and bending mode at 2511 ($2\upsilon_2 + \upsilon_4$), 1796 ($\upsilon_1 + \upsilon_4$), 875 (υ_2) and 712 (υ_4) cm^{-1} of carbonate ions relative to calcite can be detected [32,33]. The intensity of these bands increases with the increase of calcite content. For kaolin-dolomite mixtures, similar bands are observed. Compared to calcite, dolomite displays characteristic bands at 2624 and 728 cm^{-1} [34].

Whatever the mixture, after calcination at 600°C (**Figure 4 B)**, the bands of kaolinite disappear revealing the dehydroxylation of kaolin at this temperature. However, the band of carbonates persists and broadens overlapping new contributions at 1397 cm^{-1} corresponding to hydrogen carbonate HCO_3 [35] and another contribution at 1500 cm^{-1} attributed to the asymmetric stretching vibrations of carbonate groups [36]. After calcination at 750°C (**Figure 4 C)**, carbonates bands persist and in addition to that, peaks at 3700 and 3640 cm^{-1} appear due to stretching vibrations O-H of $Mg(OH)_2$ and $Ca(OH)_2$ [37,38]. These findings are in accordance with the results of thermal analysis discussed above. For kaolin-calcite mixtures, the band is composed of three contributions at 1397, 1430 and 1500 cm^{-1}. For kaolin-dolomite mixtures and especially with high dolomite content $do_{0.5}^{750}$ sample, a strong and broad band is observed in the region 1300-1600 cm^{-1} revealing structural transformations of dolomite. Indeed, the band overlaps, in addition to the contributions at 1397 and 1500 cm^{-1}, a contribution at 1450 cm^{-1} attributed to the non-decomposed dolomite and another contribution

at 1414 cm^{-1} which is related to $CaCO_3$ resulting from the decomposition of dolomite [7]. The appearance of peaks at 2521, 1800, 874 and 713 cm^{-1} confirms the formation of $CaCO_3$. To emphasize all these contributions, the intensity of the band related to hydrogen carbonate HCO_3^- at 1397 cm^{-1} normalized by the intensity of the peak of water at 1640 cm^{-1} was plotted in function of the number of moles of decomposed M^{2+} deduced from thermal analysis in **Figure 5A.** The appearance of this band is due to the partial decomposition of carbonates and their possible reaction with the air of atmosphere. In general, the intensity of hydrogen carbonate band increases with the increase of the number of moles of non-decomposed carbonates except of $do_{0.5}^{T}$ mixtures. In fact, at 600°C, for mixtures with low amount of carbonates, a low amount of M^{2+} ($1.81*10^{-5}$ and $1.53*10^{-5}$ mol for $ca_{0.1}^{600}$ and $do_{0.1}^{600}$ mixtures, respectively), corresponds to low intensity of hydrogen carbonate band (2.56 and 1.29 for $ca_{0.1}^{600}$ and $do_{0.5}^{600}$ mixtures, respectively). However, a higher content of calcite leads to the increase of decomposed M^{2+} ($7.74 *10^{-5}$ mol for $ca_{0.5}^{600}$ mixture) and therefore the increase of the normalized intensity of hydrogen carbonate bands (4.94). This is not the case of $do_{0.5}^{600}$ sample which shows a low intensity ratio (0.91). For mixtures calcined at 750°C, the same evolution is noticed except of $do_{0.5}^{750}$ sample. The mixture containing calcite and dolomite shows an intermediate position. These data suggest that a part of dolomite is surrounded of a kaolinite gangue hindering its decomposition. Similarly, the intensity of the band at 1500 cm^{-1} normalized by the intensity of the peak of water at 1640 cm^{-1} was plotted in function of the number of moles of non-decomposed M^{2+} in **Figure 5B**. This band results also from a reaction of carbonates with the air of atmosphere [39]. The same trend as observed in **Figure 5A** is obtained showing the increase of the band intensity with the increase of the number of moles of non-decomposed M^{2+} except of dolomite based mixtures $do_{0.5}^{T}$ samples). These mixtures

show low intensity of the band at 1500 cm^{-1} indicating lower formation of this carbonate which means lower reaction with the atmosphere.

Consequently, the thermal treatment at 600 and 750 °C induces partial decomposition of carbonates and the appearance of hydrogen carbonates. The decomposition of dolomite seems to be hindered by a kaolinite gangue.

In order to obtain more accurate structural information about the mixtures based on calcite and dolomite, XRD characterization was performed. The XRD patterns are presented in **Figure 6**. For kaolin-calcite mixtures, after calcination at 600°C, kaolinite peaks disappear. However, the peaks of calcite persist. The same observation is noted at 750°C with the appearance of peaks related to CaO and $Ca(OH)_2$. These data complete the results of TGA and FTIR analysis showing incomplete decomposition of calcite. For kaolin-dolomite mixtures (do_x^T), the patterns evidence also the persistence of dolomite rays at 600°C and 750°C. However, at 750°C, the intensity of dolomite decreases drastically and rays relative to calcite and MgO appear. These results also show the incomplete decomposition of dolomite at 750 °C and confirm the presence of a kaolinite gangue hindering the total decomposition of dolomite.

2) Geopolymer materials

Feasibility tests of consolidated materials were carried out for all the studied mixtures. All samples exhibit a consolidated appearance and a red-brown color due to the initial color of the used kaolin containing Fe_2O_3 [40]. However, $Gca_{0.5}^{750}$ mixture exhibits a high viscosity and a flash consolidation which can be explained by high amount of reactive calcium [41]. A gel was also observed on the surface of $Gdo_{0.5}^{600}$ sample revealing a low amount of reactive aluminium (low amount of kaolinite) and an excess of non-reacted silicate species from the alkaline solution [27]. The XRD patterns of the samples shows an amorphous dome centered at 28° characteristic of geopolymer materials as well as crystalline phases. For samples based

on calcined mixtures at 600°C, $Gca_{0.25}^{600}$ (**Figure 7A.a**) sample shows impurities of quartz, anatase and hematite from kaolin [49] and persistence of calcite. $Gca_{0.5}^{600}$ sample (**Figure 7A.b**) exhibits the same phase but with higher intensity of calcite peaks. For kaolin-dolomite mixtures based sample, dolomite and small peaks of calcite can be detected for $Gdo_{0.1}^{600}$ (**Figure 7A.c**). Less intense peaks of dolomite and more intense peaks of calcite are found in $Gdo_{0.5}^{600}$ (**Figure 7A.d**) confirming the partial decomposition of dolomite. The XRD patterns of samples based on calcined mixtures at 750°C highlight the persistence of calcite and the formation of lime and portlandite in the kaolin-calcite based geopolymers (**Figure 7C.a,b**). For kaolin-dolomite based geopolymers (**Figure 7C.c,d**), dolomite was also found in addition to the formation of calcite, MgO and $Mg(OH)_2$. In the case of kaolin-dolomite-calcite based geopolymer, (**Figure 7C.e**), dolomite, calcite, CaO, MgO, $Ca(OH)_2$ and $Mg(OH)_2$ are detected.

Consequently, consolidated materials were successfully obtained from the different mixtures of kaolin and carbonates calcined at 600 and 750°C. The mineral composition shows the coexistence of an amorphous geopolymer network, residual non-decomposed carbonates and reactive alkali earth cations resulting from decomposed carbonates.

b. Thermal behavior

In order to evaluate the thermal behavior of the synthesized geopolymers, they were heated at 1000°C. Then, X- ray diffraction was performed to identify the mineralogical changes. The chemical composition and the PDF files of the different mineral phases are reported in **supplementary file.** Whatever the sample, crystalline phases can be detected. $Gca_{0.1}^{600}$ sample (**Figure 7B.a'**) shows the persistence of quartz and the formation of leucite $K(AlSi_2O_6)$ and wollastonite ($CaSiO_3$). The formation of leucite ($KAlSi_2O_6$) was previously evidenced in potassium based geopolymers [42,43]. Its formation is favored at higher temperature (>800°C) and higher Si/Al molar ratio. Wollastonite was also found in the work

of Dupuy et al.[24] and results from a reaction at 780°C between silica from the amorphous phase and available calcium from carbonate decomposition [44]. With the increase of calcite content in $Gca_{0.5}^{600}$ sample (**Figure 7B.b'**), the quartz peaks intensity decreases drastically and more wollastonite is formed to the detriment of leucite and kalsilite due to higher available calcium. Furthermore, others calcium silicates are formed such as Ca_2SiO_4 (α C2S) calico-olivine (γ C2S), larnite (β C2S). Indeed, Larnite can be formed from a reaction between quartz and lime from a temperature of 930 °C [45]. Calcio-olivine is the stable Ca_2SiO_4 polymorph and is formed according to literature during cooling to room temperature [48]. No differences can be detected for kaolin – dolomite based samples (**Figure 7D. c'and d').**

The same phases as at 600°C are detected for samples based on mixtures calcined at 750°C (**Figure 7D. a',b' and c'**) except of $Gdo_{0.5}^{750}$ sample (**Figure 7D.d'**) showing the formation of additional phases such as akermanite ($Ca_2MgSi_2O_7$), merwinite ($Ca_3Mg(SiO_4)_2$) and potassium magnesium silicate due to higher availability of magnesium and calcium. In the case of kaolin-dolomite-calcite based geopolymer (**Figure 7D.e'**), quartz, leucite, kalsilite, merwinite wollastonite and calico-olivine are detected.

In summary, the thermal treatment at 1000°C leads to the formation of crystalline phases which depend on the initial chemical composition of the mixture. In fact, the amorphous phase crystallizes to form potassium aluminium silicate, kalsilite and /or leucite. At lower content of alkaline earth species (Ca^{2+} and Mg^{2+}), only wollastonite is formed. However, at higher content different calcium and magnesium silicates can be formed.

Dilatometry measurements and DTA-TGA thermal analysis have been also carried on the geopolymer samples. The shrinkage curves as well as the TGA curves of the samples are presented in **Figure 8**. For kaolin –calcite based samples calcined at 600 °C, for $Gca_{0.1}^{600}$ a very small shrinkage (1%) is observed until 200°C and associated to an important weight loss

of 19.6 % and is due to the release of free and physisorbed water [46]. Then, a shrinkage of 1.5 % is detected until 800°C and can be attributed to the release of hydroxyl groups on the surface [47]. The TGA curve shows a weight losses of 2.2 % between 600 and 800°C attributed to the decomposition of the remaining calcite. A major shrinkage of 9.7 %, not accompanied by a weight loss, is observed between 800 and 1000°C and attributed to two phenomena i) the formation of a viscous flux and the ii) crystallization of crystalline phases from 900°C which can be wollastonite and leucite according to XRD data [48]. A different shrinkage curve is observed in the case of $Gca_{0.5}^{600}$ sample with an expansion between 600°C to 800°C followed by a shrinkage of 5 % between 800 and 1000°C. The expansion is may be due to the decomposition of carbonates. In fact the corresponding TGA curve shows three weight losses of about 2.6, 2.9 and 8.6% in the temperature ranges 500-550, 550-650 and 650-800°C, respectively. In order to identify the different weight losses, mass spectrometry coupled with thermal analysis was performed. Only the obtained curve relative to the mass/charge ratio (m/z) of 44 corresponding to the release of CO_2 is given in **supplementary file**. As expected, three contributions of CO_2 between 500-550, 550-650 and 650-800°C are shown. This results confirms the decomposition of three types of carbonates with different crystallinities which can be attributed to hydrogen bicarbonate [49], mixed carbonates and calcite. The hydrogen bicarbonate results from the interaction with humidity of the air and the mixed carbonates from the exchange of alkali and alkali earth cations [52]. A slightly higher total shrinkage (15 %) is observed in the case of $Gdo_{0.1}^{600}$ sample. This is not the case of $Gdo_{0.5}^{600}$ sample showing the lowest shrinkage value (6.9 %). Three weight losses were also observed in the TGA curves of 2.6, 4.0 and 6.5% in the temperature ranges 500-550, 550-650 and 650-800°C respectively. The formation of viscous flux begins at lower temperature (712°C). This is due to the presence of a higher amount of alkali-earth cations (Ca^{2+} and Mg^{2+}) acting as flux lowering the viscous flux temperature [50]. At 750 °C, similar shrinkage

curves are observed except of $Gca_{0.5}^{750}$ showing an expansion from 600°C to 800°C then a shrinkage of 4 % between 800 and 1000°C. The expansion could be explained by on one hand the higher carbonate content which decomposes between 600 and 800°C and on the other hand the elimination of residual stress caused by the flash consolidation of this sample such as in glasses [51]. The TGA curve presents three weight losses (4.2, 3.7 and 6.4 in the temperature ranges 500-550, 550-650 and 650-800°C respectively) corresponding to the decomposition of hydrogen bicarbonate [52], mixed carbonates and calcite as previously demonstrated. Once again, $Gdo_{0.75}^{750}$ shows a low shrinkage (8%) and the formation of viscous flow and the crystallization of crystalline phases of lower temperature (700 and 800°C respectively). This results is in accordance with XRD data and literature showing crystallisation of akermanite and merwinite at 850°C [53,54]. The TGA curve shows also three weight losses of 2.6, 2.9 and 2.8% between 500-550, 550-650 and 650-800°C, respectively.

The total shrinkage is plotted in function of the viscous flux temperature determined from the first derivative of the shrinkage curve (maximum of viscous flux) (**Figure 9A**). In order to validate the correlations, three extra formulations previously studied have been added, one based on kaolin and argillite calcined at 750°C [26] and two formulation based on metakaolin and Moroccan clays rich in carbonates [55]. The formulations were also added in the CaO-MgO-$2SiO_2Al_2O_3$ ternary diagram (see supplementary file). A linear correlation is evidenced showing the increase of the shrinkage value from 6 to 15.6% with the increase of viscous flux temperature from 687 to 922 °C for $Gca_{0.5}^{750}$ and $Gdo_{0.1}^{600}$ samples respectively. The shrinkage and the temperature of viscous flow are low for $Gca_{0.5}^{T}$ and $Gdo_{0.5}^{T}$ samples. This fact can be explained in the first case by the formation of different calcium silicate compounds as demonstrated by XRD lowering the shrinkage. In the second case, for high dolomite content based samples $Gdo_{0.5}^{T}$, the presence of magnesium lowers the viscous flow

temperature. The silica is consumed for the formation of magnesium and calcium silicate and will not be available to form a liquid phase which decreases the shrinkage [56]. Higher shrinkage values and viscous flow temperature are obtained for low carbonates content based samples ($Gca_{0.1}^{T}$ and $Gdo_{0.1}^{T}$). Indeed, silica from the amorphous phase remains free leading to higher liquid phase and thus higher shrinkage. In order to verify this result, the shrinkage values were also plotted in function of the molar ratio of the remaining M^{2+} in geopolymer samples determined from TGA analysis (weight loss between 500-800°C) and the M^{2+} initially present in the raw mixtures (**Figure 9B**). It is shown a decrease of the shrinkage in function of this ratio. For low carbonates content samples, whatever the calcination temperature, the molar ratios varies between 0.06 and 0.13 with shrinkage values between 15 and 12% which corresponds to $Gdo_{0.1}^{600}$ and $Gca_{0.1}^{750}$ samples. For high carbonates content samples, the molar ratios varies between 0.18 and 0.44 between which corresponds to a low shrinkage value varying between 6 and 8 % for $Gca_{0.5}^{750}$ and $Gdo_{0.5}^{750}$ samples, respectively. Indeed, the increase of available alkaline earth cations leads to the creation of non-bridging oxygens NBO and disorder favoring the formation of crystalline phases [57]. In fact, they will react at high temperature to form calcium and/or magnesium silicates which reduces the shrinkage. SEM photos at the temperature of viscous flux temperature appearance (**Figure 9A**) and at 1000°C are reported in **Figure 10**. Three examples of sample were selected. For low carbonates content such as $Gdo_{0.1}^{750}$ sample (**Figure 10a**) exhibiting high viscous flux temperature and high shrinkage (878°C and 12 % respectively), the observed microstructure is similar to typical metakaolin based geopolymer showing glass-like structure with high porosity content [58]. For $Gca_{0.13}do_{0.05}^{750}$ sample (**Figure 10b**), having intermediate values of viscous flux temperature and shrinkage (813°C and 10% respectively) it is observed the sintering of the amorphous phase and also the appearance of crystals and fibrous particles. For high carbonate content such as $Gca_{0.5}^{750}$ sample (**Figure 10c**) characterized by low viscous

flux temperature and shrinkage value (687°C and 6 % respectively). More heterogeneous microstructure is observed indicating the formation of different crystalline phases. These observations corroborate the data in Figure **9.** Consequently, it is possible to control the thermal shrinkage by the control of the carbonates content (nM^{2+}) in the geopolymer and the well knowledge of the raw materials.

Conclusion

This study aims to propose a model of thermal behaviour of geopolymer materials by investigating the effect of carbonate nature and amount and the calcination temperature of the aluminosilicate source. For this, two mixtures of kaolin and calcite (10 and 50 wt.% of calcite), two mixtures of kaolin and dolomite (10 and 50 wt.% of dolomite) calcined at 600 and 750°C and a mixture composed of kaolin, dolomite (5 wt.%) and calcite (13 wt.%) calcined at 750°C were studied. The characterization of these mixtures by thermal analysis, FTIR spectroscopy and XRD evidenced the complete dehydroxylation of kaolin and the persistence of carbonates after calcination at 600°C. Partial decomposition of calcite and dolomite was proven after calcination at 750°C. Furthermore, it was demonstrated that a kaolinite gangue can hinder the decomposition of dolomite in the case of mixture composed of 50 wt. % of dolomite. Then, the thermal behavior at 1000°C of the obtained consolidated materials based on these mixtures was evaluated. Two different behaviours can be distinguished:

i) Geopolymers based on low carbonates content exhibit high shrinkage (from 12 to 16%) and viscous flow at high temperature. They are characterized by the formation of potassium aluminium silicate, kalsilite, leucite and wollastonite.

ii) Geopolymers based on high carbonates content exhibit lower shrinkage (from 6 to 8%), the appearance of viscous flow at lower temperature and the crystallisation of different additional phases (calcium and/or magnesium silicates).

Acknowledgment

Project supported by Andra under the "Investing in the Future Programme" ("Investissement d'Avenir") - Selected under the Andra Call for Projects: "Optimisation of post-dismantling radioactive waste management", organised in cooperation with the French National Research Agency (ANR).

References

[1] J. Davidovits, Geopolymers, inorganic polymeric new materials, J.Therm. Anal. 37 (1991) 1633-1656.

[2] K.J.D. MacKenzie, , What are these things called geopolymers? A physico-chemical perspective. Adv. Ceram. Matrix Composites IX, Ceram. Trans. 153 (2003) 175–186.

[3] K.J. D. MacKenzie, Inorganic polymers (geopolymers), In Encyclopedia of Polymer Science and Technology, Wiley (2017) 1-31. DOI:10.1002/0471440264.pst165.pub2. ISBN 9780471440260.

[4] Y.M Liew, H. Kamarudin, A.M. Mustafa Al Bakri, M. Luqman, I . Khairul Nizar, C.Y. Heah. Investigating the possibility of utilization of kaolin and the potential of metakaolin to produce green cement for construction purposes. Aust J Basic Appl Sci. 5 (2011) 441–9.

[5] A. Buchwald, M. Hohman, K. Posern, and E. Brendler. The suitability of thermally activated illite/smectite clay as raw material for geopolymer binders. Appl. Clay. Sci. 46 (2009) 300–304.

[6] X.Yao, Z. Zhang, H. Zhu, and Y.Chen. Geopolymerization Process of Alkali-Metakaolinite Characterized by Isothermal Calrimetry. Thermochim. Acta. 493 (2009) 49–54.

[7] A. K. Galwey, M. E. Brown, Chapter 12 Decomposition of carbonates, Studies in Physical and Theoretical Chemistry 86 (1999) 345-364.

[8] A. R. Salvador, E.G. Calvo, C.B. Aparicio, Effects of sample weight, particle size, purge gas and crystalline structure on the observed kinetic parameters of calcium carbonate decomposition, Thermochim. Acta. 143 (1989) 339-345.

[9] K.S.P. Karunadasa, C.H. Manoratne, H.M.T.G.A. Pitawala, R.M.G. Rajapakse, Thermal decomposition of calcium carbonate (calcite polymorph) as examined by in-situ high-temperature X-ray powder diffraction, J. Phys. Chem. Solids. 134 (2019) 21-28.

[10] A.I. Rat'ko, A.I. Ivanets, A. I. Kulak, E.A. Morozov, I.O. Sakhar, Thermal decomposition of natural dolomite, Inorg. Mater. 47 (2011) 1372-1377.

[11] R.C. Mackenzie, A.A. Rahman, Interaction of kaolinite with calcite on heating: I. instrumental and procedural factors for one kaolinite in air and nitrogen, Thermochim. Acta. 121 (1987) 51-69,

[12] R.C. Mackenzie, A.A. Rahman, H.M. Moir, Interaction of kaolinite with calcite on heating. II. mixtures with one kaolinite in carbon dioxide, Thermochimic. Acta. 124 (1988) 119-127.

[13] R. S. Mitchell, S.C. Hart, Heated Mineral Mixtures Related to Ancient Ceramic Pastes X-ray Diffraction Study, Archaeological Chemistry IV, 1989, pp 145-155

[14] J. Zhou, X. Zhang, Y. Wang, A. Larbot, X. Hu, Elaboration and characterization of tubular macroporous ceramic support for membranes from kaolin and dolomite, J. Porous Mater. 17 (2010) 1-9.

[15] A.S. Sauffi, W.M.W. Ibrahim, R. Ahmad, N.A.M. Mortar, F.A. Zaidi & W.W.A. Zailani, A review of morphology analysis on dolomite as an additive material in geopolymer, IOP Conf. Series : Mater.Sci. Eng. 743 (2020) 012024.

[16] E.A. Aizat, A.M.M. Al Bakri, Y.M. Liew, C.Y. Heah, Chemical composition and strength of dolomite geopolymer composites, AIP Conference Proceedings, 1885 (2017) 020192.

[17] A.S. Ouda, M. Gharieb, Development the properties of brick geopolymer pastes using concrete waste incorporation dolomite aggregate, J. Build. Eng. 27 (2020) 1-12.

[18] A. Aboulayt, M. Riahi, M. Ouzzani Touhami, H. Hannache, M. Gomina, R. Moussa, Properties of metakaolin based geopolymer incorporating calcium carbonate, Adv. Powder Technol. 28 (2017) 2393 -2401.

[19] N. Kutuk, S. Cetinkaya, Effect of kaolinite mass ratio on compressiove strength of kaolinite-calcite based geopolymer, International Journal of Computation and Experimental Science and Engineering. 3 (2017) 25-28.

[20] C.K. Yip, J.L. Provis, G.C. Lukey, J.S.J. van Deventer, Carbonate mineral addition to metakaolin-based geopolymers, Cem. Concr. Compos. 30 (2008) 979-985,

[21] L. Valentini, S. Contessi, M.C. Dalconi, F. Zorzi, E. Garbin, Alkali-activated calcined smectite clay blended with waste calcium carbonate as a low-carbon binder, J. Clean. Prod. 184 (2018) 41-49.

[22] E.A. Azimi, M.M.A.B. Abdullah, L.Y. Ming, H.C. Yong, K. Hussin, I.H. Aziz, Review of dolomite as precursor of geopolymer materials. MATEC Web of Conferences, 78 (2016) 01090.

[23] A. Natali Murri, W.D.A. Rickard, M.C. Bignozzi, A. van Riessen, High temperature behaviour of ambient cured alkali-activated materials based on ladle slag, Cement. Concrete. Res. 43 (2013) 51-61.

[24] C. Dupuy, A. Gharzouni, N. Texier-Mandoki, X. Bourbon, S. Rossignol, Alkali-Activated Materials Based on Callovo-Oxfordian Argillite: Formation, Structure and Mechanical Properties, J. Ceram. Sci. Technol. 9 (2018) 127-140, DOI: 10.4416/JCST2017-0008

[25] C. Dupuy, A. Gharzouni, I. Sobrados, N. Texier-Mandoki, X. Bourbon, S. Rossignol, Thermal resistance of argillite based alkali-activated materials. Part 2: Identification of the formed crystalline phases, Mater. Chem. Phys. 218 (2018) 262-271.

[26] S.Yan, F. Zhang, S. Wang, P. He, D.Jia, J. Yang, Crystallization behavior and mechanical properties of high open porosity dolomite hollow microspheres filled hybrid geopolymer foams, Cem. Concr. Compos. 104, (2019) 103376.

[27] M.Tognonvi, S. Petlitckaia, A.Gharzouni, M.Fricheteau, N. Texier-Mandoki, X. Bourbon, S. Rossignol, High-temperature, resistant, argillite based, alkali activated materials with improved post-thermal treatment mechanical strength. Clays Clay Miner. 68 (2020) 211–219.

[28] A. Gharzouni, (2016). Contrôle de l'attaque des sources aluminosilicates par la compréhension des solutions alcalines. PhD. thesis, University of Limoges, Limoges, France, pp 227.

[29] P. Djomgoue, D. Njopwouo, FT-IR Spectroscopy Applied for Surface Clays Characterization, J. Surf. Eng. Mater. Adv. Technol. 3 (2013) 275-282.

[30] J. Madejova, FTIR techniques in clay mineral studies. Vib.Spectrosc. 31(2003) 1 –10.

[31] S. K. Petrovskii, O. G. Stepanova, S. S. Vorobyeva, T. V. Pogodaeva, A. P. Fedotov, The use of FTIR methods for rapid determination of contents of mineral and biogenic components in lake bottom sediments, based on studying of East Siberian lakes, Environ. Earth. Sci. 75 (2016) 226.

[32] S. Gunasekaran, G. Anbalagan,Spectroscopic characterization of natural calcite minerals, Spectrochimica Acta Part A: Molecular and Biomolecular Spectroscopy. 68(2007) 656-664.

[33] HuaNc, C., Konn, P. Infrared study of the carbonate minerals. Am. Miner.45 (1960) 371 -324.

[34] J. Ji, Y. Ge, William Balsam, J. E. Damuth, Jun Chen,Rapid identification of dolomite using a Fourier Transform Infrared Spectrophotometer (FTIR): A fast method for identifying Heinrich events in IODP Site U1308, Marine Geology, 258 (2009) 60-68.

[35] E.M Köck, M. Kogler, T. Bielz, B. Klötzer, S. Penner, In Situ FT-IR Spectroscopic Study of CO_2 and CO Adsorption on Y_2O_3, ZrO_2, and Yttria-Stabilized ZrO_2, J. Phys. Chem. C 2013, 117, 34 (2013) 17666-17673.

[36] A. Grzechnik, H. D. Zimmermann, R. L. Hervig, P. L. King, P.F. McMillan, FTIR micro-reflectance measurements of the CO_3^{2-} ion content in basanite and leucitite glasses, Contrib. Mineral. Petrol. 125 (1996) 311–318.

[37] M. Khachani, A. El Hamidi, M. Halim, S. Arsalane Non-isothermal kinetic and thermodynamic studies of the dehydroxylation process of synthetic calcium hydroxide $Ca(OH)_2$, J. Mater. Environ. Sci. 5 (2) (2014) 615-624

[38] A. Pilarska, M.Wysokowski, E. Markiewicz, Teofil Jesionowski, Synthesis of magnesium hydroxide and its calcinates by a precipitation method with the use of magnesium sulfate and poly(ethylene glycols), Powder Technol. 235 (2013) 148-157

[39] A. K. Pathak, T. Mukherjee and D. K. Maity, IR Spectra of Carbonate-Water Clusters, CO_3^{-2} $(H_2O)_n$: A Theoretical Study, Synthesis and Reactivity in Inorganic, Metal-Organic, and Nano-Metal Chemistry, 38(2008)76–83

[40]A. Gharzouni, I. Sobrados, E. Joussein, S. Baklouti, S. Rossginol, Control of polycondensation reaction generated from different metakaolin and alkaline solution, J. Ceram. Sci. Technol., 8 (2017) 365-376, 10.4416/JCST2017-00040

[41] C. Dupuy, A. Gharzouni, N. Mandoki, X. Bourbon, S. Rossginol, Alkali-Activated Materials based on Callovo-Oxfordian Argillite: Formation, Structure and Mechanical Properties, J. Ceram. Sci. Technol., 9(2) (2018) 127-140

[42] V. F.F. Barbosa, K.J.D. MacKenzie, Synthesis and thermal behaviour of potassium sialate geopolymers, Mater. Lett. 57 (2003) 1477-1482.

[43] P. Duxson, G.C. Lukey, J.S.J. van Deventer, The thermal evolution of metakaolin geopolymers: Part 2 – Phase stability and structural development. J. Non-Cryst. Solids. 353 (2007) 2186-2200.

[44] Q. Yu, K. Sawayama, S. Sugita, M. Shoya, Y. IsojimaThe reaction between rice husk ash and Ca(OH)2 solution and the nature of its product, Cement Concr. Res., 29 (1999), pp. 37-43

[45] N. Bohme, K. Hauke, M. Neuroth, T. Geisler, In situ Raman imaging of high-temperature solid-state reactions in the $CaSO_4$–SiO_2 system, Int. J. Coal. Sci. Technol. 6(2) (2019) 247–259.

[46] W. Rickard, A. van Riessen, J. Temuujin, Thermal analysis of geopolymer pastes synthesised from five fly ashes of variable composition, J. Non-Cryst. Solids. 358 (2012) 1830-1839.

[47] P. Duxson, G.C. Lukey, J.S.J. van Deventer, Physical evolution of Na-geopolymer derived from metakaolin up to 1000 °C. J Mater Sci. 42 (2007) 3044–3054

[48] J.L. Bell, P.E. Driemeyer and W.M. Kriven, Formation of Ceramics from Metakaolin-Based Geopolymers. Part II: K-Based Geopolymer. J. Am. Ceram. Soc. 92 (2009) 607-615.

[49] I. C. Hisatsune and T. Adi, Thermal Decomposition of Potassium Bicarbonate, J. Phys. Chem. 74 (1970) 2875–2877.

[50] C. Dupuy, Valorisation de l'argilite du Callovo-Oxfordien sous forme de liant alcalinement activé dans le but de développer un coulis injectable PhD. thesis, University of Limoges, Limoges, France, 2019.

[51] J. Zarzycki, Glasses and the vitreous state, Cambridge University Press, 1991.

[52] I. C. Hisatsune and T. Adi, Thermal Decomposition of Potassium Bicarbonate, J. Phys. Chem. 74 (1970) 2875–2877.

[53]Y. J. Zhang, S. Li, Y.Chao Wang, D. L. Xu, Microstructural and strength evolutions of geopolymer composite reinforced by resin exposed to elevated temperature, J. Non-Cryst. Solids, 358, (2012) 620-624.

[54] M. Mohabbi Yadollahi & Murat Dener, Investigation of elevated temperature on compressive strength and microstructure of alkali activated slag based cements, European Journal of Environmental and Civil Engineering, (2019) DOI: 10.1080/19648189.2018.1557562

[55] A.El Khomsi, A. Gharzouni, N. Kandri, A. Zerouale, S. Rossignol, Properties of Geopolymer Composites from two Different Moroccan Clays. Ceramics in Modern Technologies. 2 (2020)10.29272/cmt.2020.0001.

[56] Claudia Lira, Marcio C. Fredel, Mauro D. M. da Silveira, Orestes E. Alarcon, Effect of carbonates on firing shrinkage and on moisture expansion of porous ceramics tiles. (1998)10.13140/2.1.2102.3522.

[57] Reddy, A.A., Tulyaganov, D.U., Kharton, V.V. et al. Development of bilayer glass-ceramic SOFC sealants via optimizing the chemical composition of glasses—a review. J Solid State Electrochem. 19 (2015) 2899–2916. https://doi.org/10.1007/s10008-015-2925-5

[58] P. Payakaniti, N. Chuewangkam, R. Yensano, S. Pinitsoontorn, P.Chindaprasirt, Changes in compressive strength, microstructure and magnetic properties of a high-calcium fly ash geopolymer subjected to high temperatures, Constr. Build. Mater. 265 (2020) 120650.

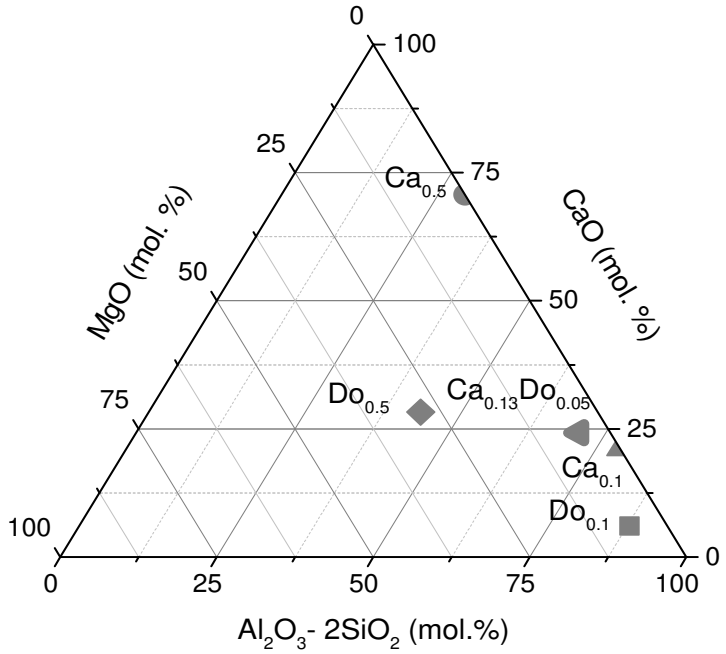

Figure 1 : Chemical composition of the mixtures ca_xdo_y in the CaO – MgO – Al_2O_3-$2SiO_2$ ternary diagram $ca_{0.1}$ (▲), $ca_{0.5}$ (●), $do_{0.1}$ (■), $do_{0.5}$ (♦) and $ca_{0.13}do_{0.05}$ (◄)

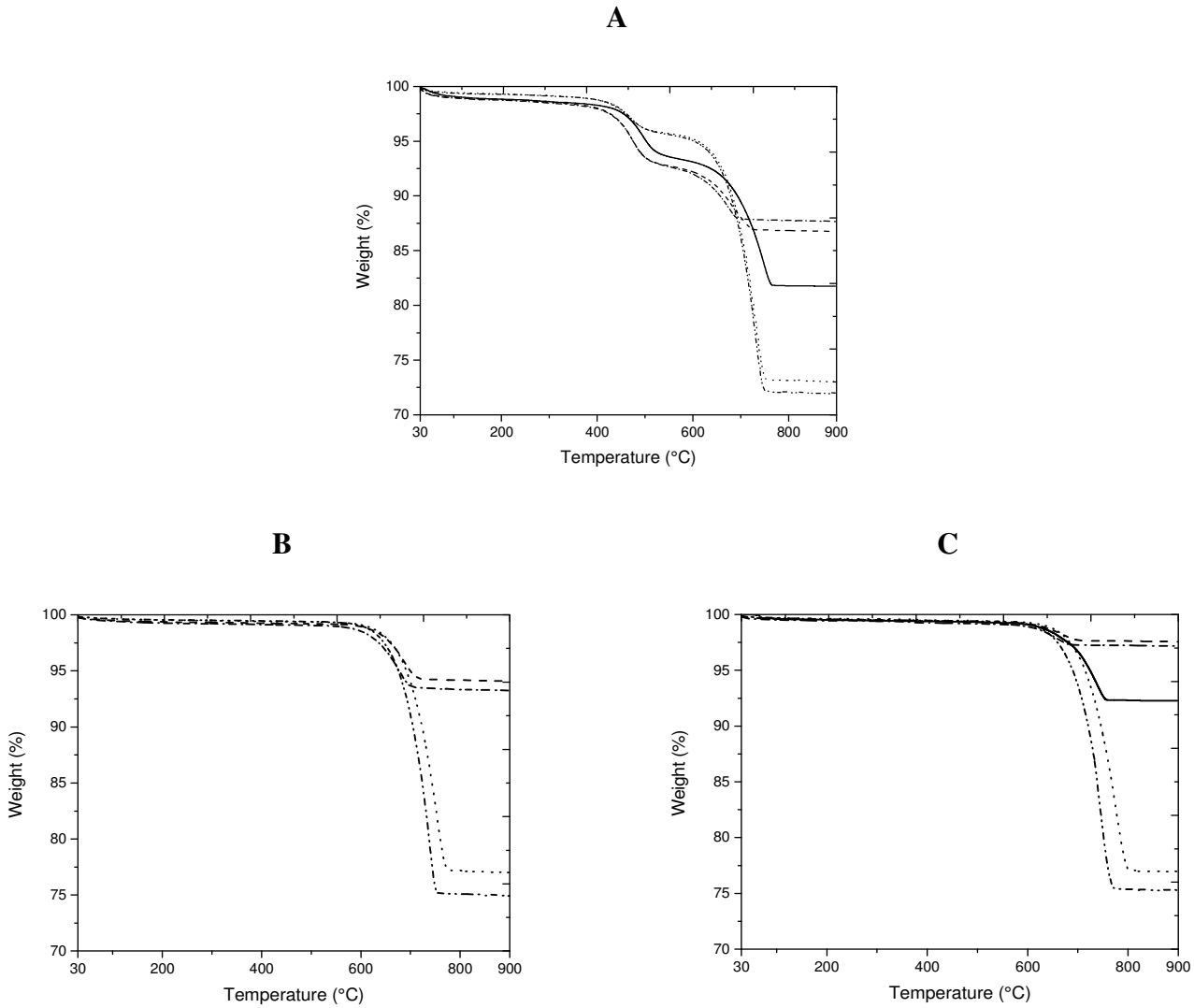

Figure 2 : TGA curves of $ca_xdo_y^T$ mixtures (A) before and after calcination at (B) 600 and (C) 750 °C for $ca_{0.1}$ (---), $ca_{0.5}$ (…), $do_{0.1}$ (-.-.-), $do_{0.5}$ (-..-..-), $ca_{0.13}do_{0.05}$ (—)

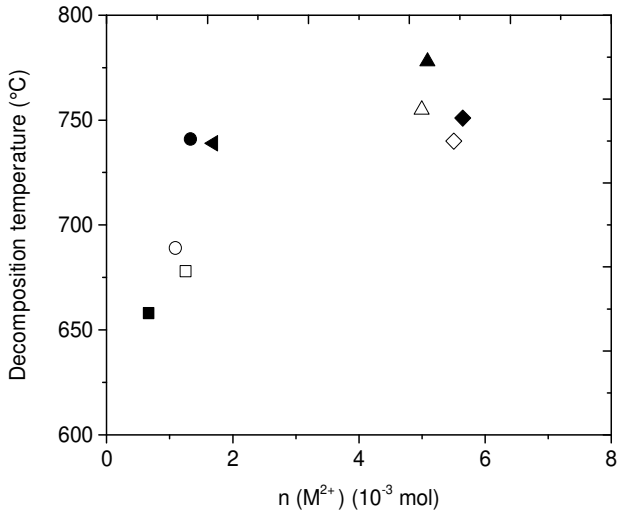

Figure 3 : Value of decomposition temperature of carbonates of $ca_xdo_y^T$ mixtures calcined at 600 (empty) and 750 °C (black) ($ca_{0.1}$ (○, ●), $ca_{0.5}$ (Δ,▲),$do_{0.1}$ (□, ■), $do_{0.5}$ (◊,♦); $ca_{0.13}do_{0.05}$ (◄))

A

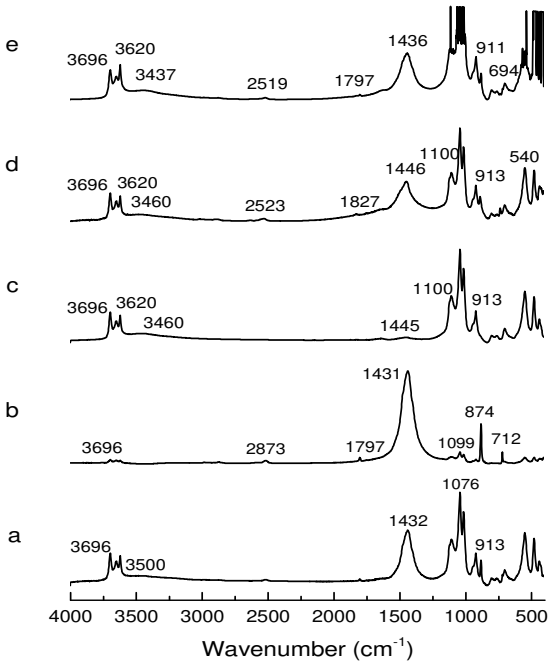
e
3696
3620
3437
2519
1797
1436
911
694
d
3696
3620
3460
2523
1827
1446
1100
913
540
c
3696
3620
3460
1445
1100
913
b
3696
2873
1797
1431
1099
874
712
a
3696
3500
1432
1076
913
4000
3500
3000
2500
2000
1500
1000
500
Wavenumber (cm-1)

B C

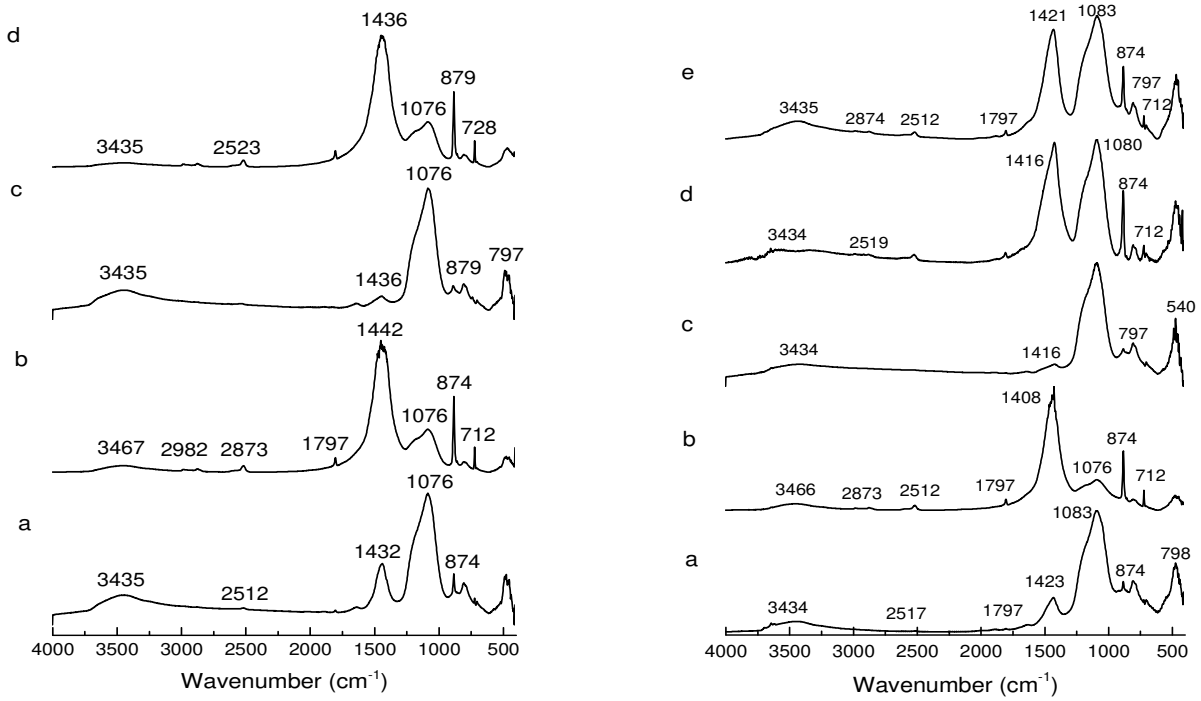

Figure 4 **:** FTIR spectra of mixtures $ca_xdo_y^T$ (A) non-calcined, calcined at (B) 600 and (C) 750°C (with (a) $ca_{0.1}$, (b) $ca_{0.5}$, (c) $do_{0.1}$, (d) $do_{0.5}$ and (e) $ca_{0.13}do_{0.05}$)

A

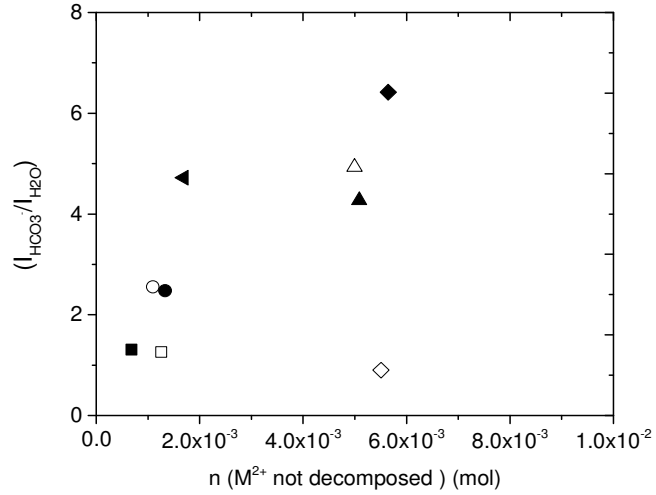

B

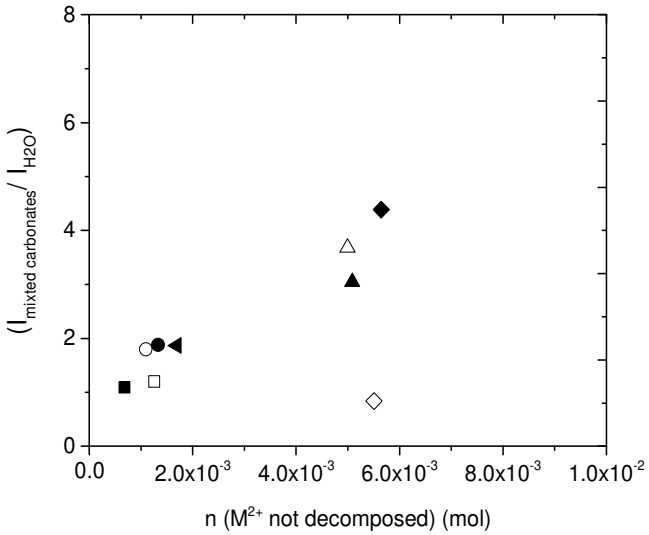

Figure 5 : Ratio of $\frac{I_{HCO3}\,(1397\ cm{-}1)}{I_{H2O}\,(1620\ cm{-}1)}$ (A) and $\frac{I_{mixed\ carbonates}\,(1500\ cm{-}1)}{I_{H2O}\,(1620\ cm{-}1)}$ (B) for the mixtures ca_xdo_y T calcined at 600 °C (empty) and 750 °C (black) ($ca_{0.1}$ (○,●), $ca_{0.5}$ (Δ,▲), $do_{0.1}$ (□,■), $do_{0.5}$(◊,♦) and $ca_{0.13}do_{0.05}$ (◀).

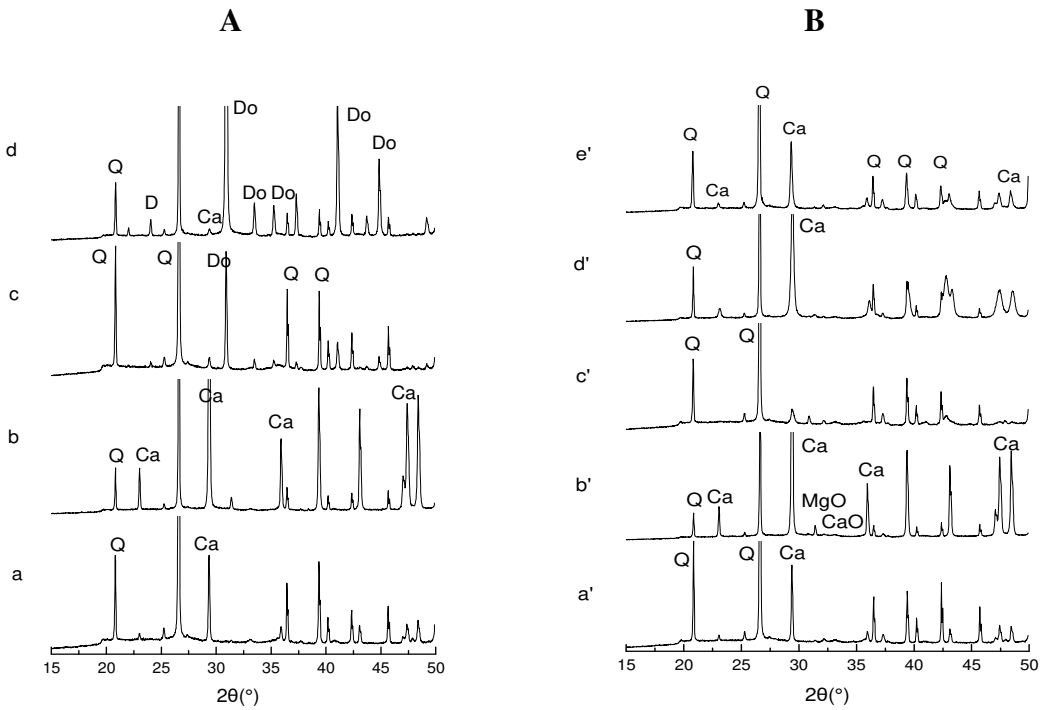

Figure 6 : XRD patterns of mixtures $ca_xdo_y^T$ where $ca_{0.1}$(a, a'), $ca_{0.5}$(b, b'), $do_{0.1}$(c, c'), $do_{0.5}$(d, d') and $ca_{0.13}do_{0.05}$ (e, e') calcined at (A) 600 and (B) 750 °C *(Q-quartz, Ca-calcite, Do-dolomite)*

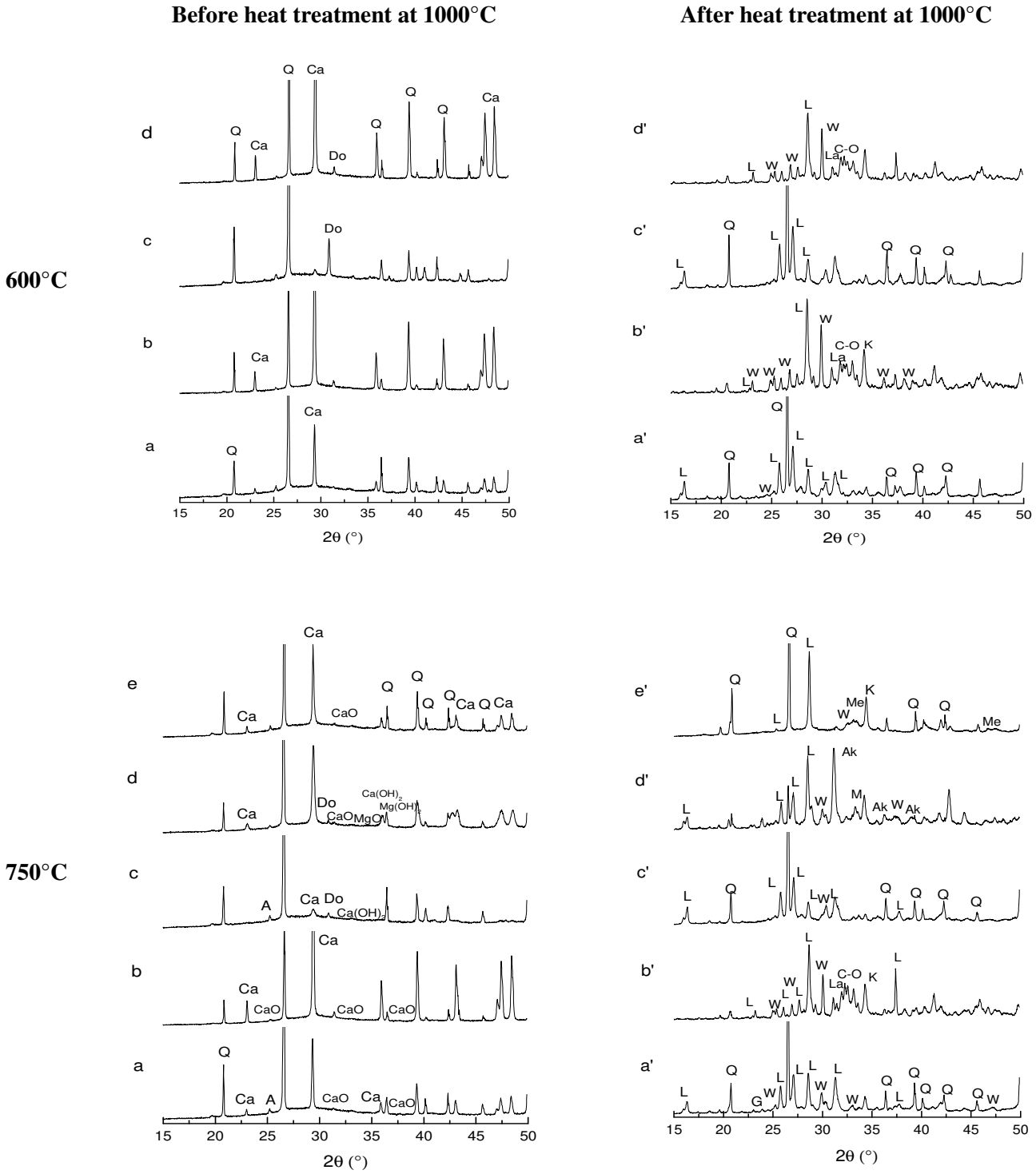

***Figure 7**:* XRD patterns of geopolymers $Gca_xdo_y^T$ based on the mixtures (a, a') $ca_{0.1}$, $ca_{0.5}$, (b, b') $do_{0.1}$, (c, c'), (d, d') $do_{0.5}$ and (e, e') $ca_{0.13}do_{0.05}$ calcined at 600°C and 750°C before and after heat treatment at 1000 °C (*Q-quartz, Ca-calcite, Do-dolomite, A-anatase, L-leucite, G-gehlenite, W-wollastonite, C-O – calcio-olivine, La-larnite, K-kalsilite, Me – merwinite, Ak - akermatite)*

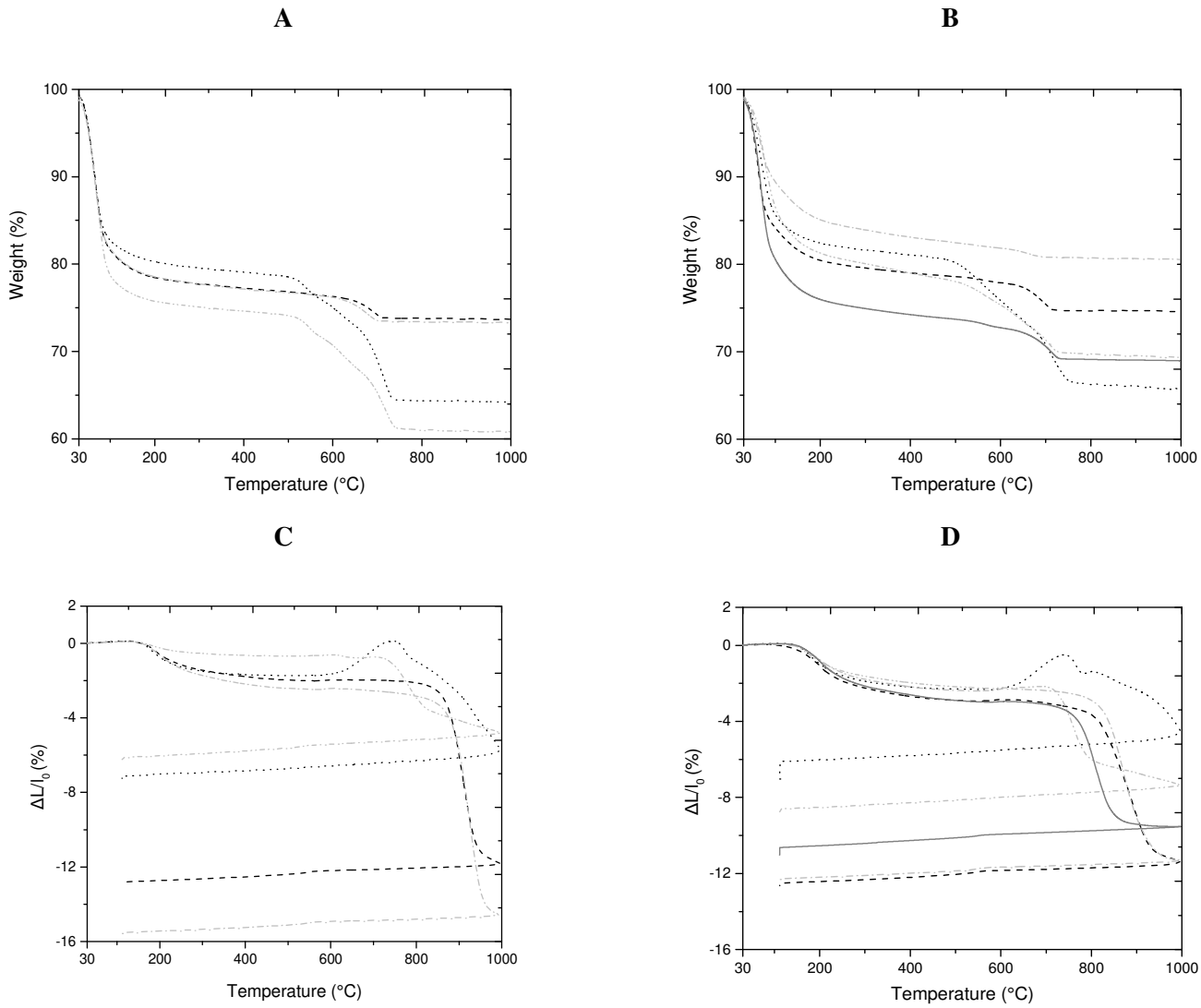

Figure 8: (A, B) TGA and (C, D) dilatometric curves of geopolymers samples based on the mixture $Ca_xDo_y^T$ calcined at (A, C) 600 and (B, D) 750°C with $ca_{0.1}$ (---), $ca_{0.5}$ (…), $do_{0.1}$ (-.-.-), $do_{0.5}$ (-..-..-) and $ca_{0.13}do_{0.05}$ (—).

A

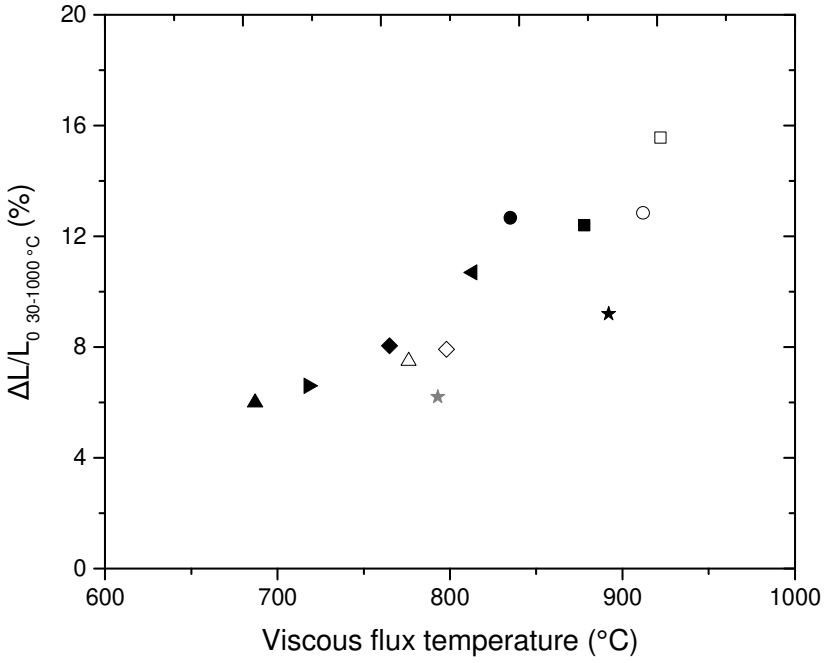

B

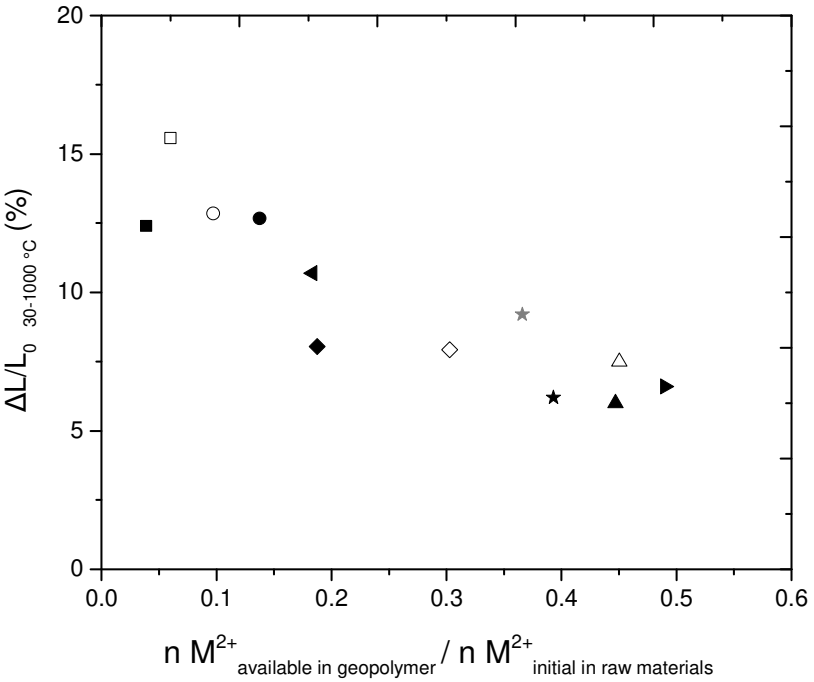

Figure 9: Value of shrinkage between 30 and 1000 °C of geopolymer samples $G(ca_xdo_y)^T$ based on the mixtures calcined at 600 °C (empty) and 750 °C (black) ($ca_{0.1}$ (○,●), $ca_{0.5}$ (Δ,▲), $do_{0.1}$ (□,■), $do_{0.5}$(◊,♦) and $ca_{0.13}do_{0.05}$ (◄) and extra formulations (►) from [26] and (★, ★) from [57] in function of (A) viscous flux temperature and (B) the molar ratio (nM^{2+}available in geopolymers/ nM^{2+} initial in raw materials)

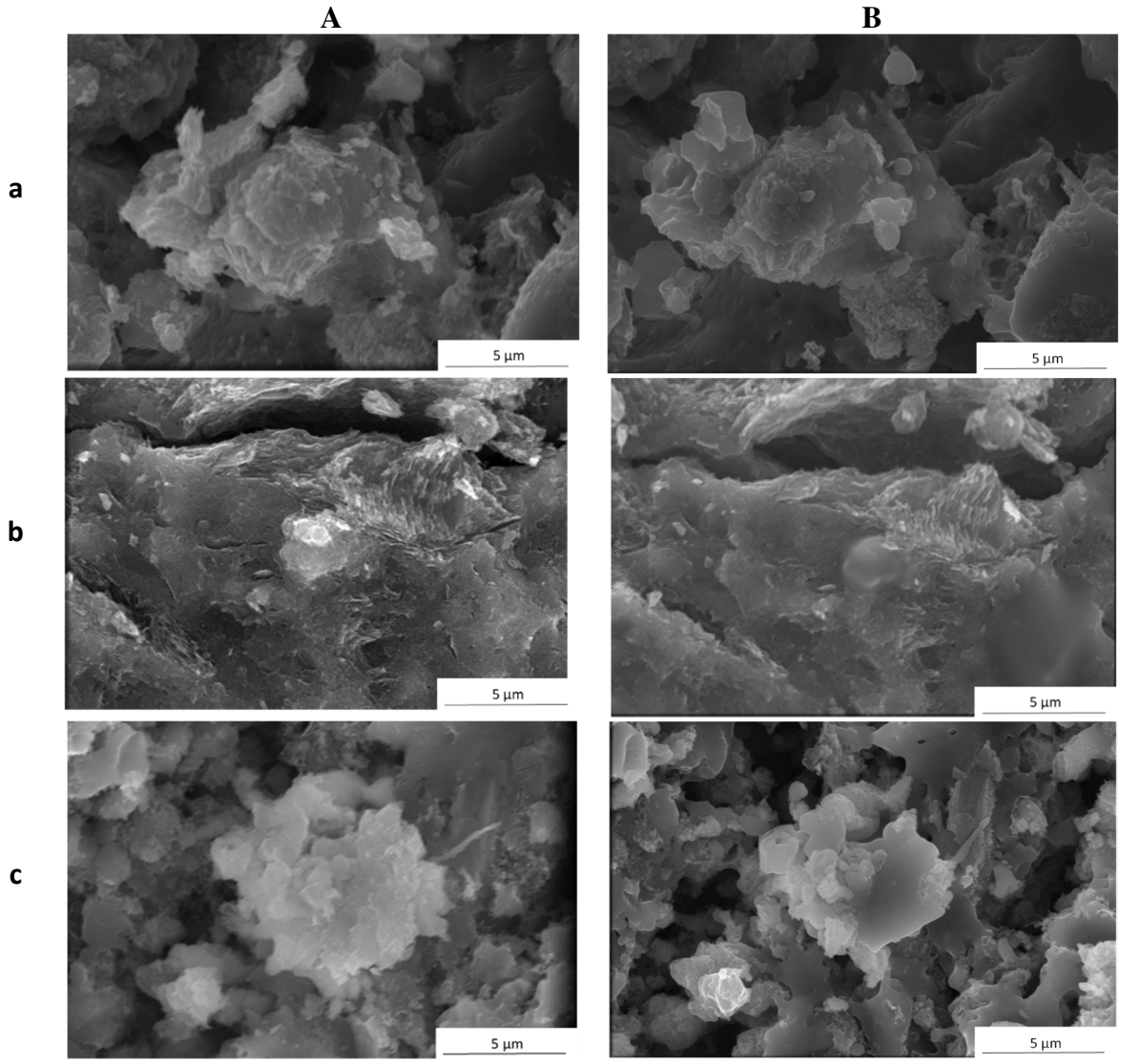

Figure 10: SEM images of geopolymer samples at (A) the temperature of viscous flux appearance and (B) at 1000 °C for (a) $Gdo_{0.1}^{750}$, (b) $Gca_{0.13}do_{0.05}^{750}$ and (c) $Gca_{0.5}^{750}$

Table 1. Chemical and physical characteristics of uses raw materials

Raw materials	**Supplier**	**D_{50} (µm)**	**S_{BET} (m^2/g)**	**Water demand (µL/g)**
Kaolin	Argeco (France)	20	24	530
Calcite	Ceradel (France)	2	2	310
Dolomite		14	1	273

Table 2: Values of decomposition temperature and loss of masse according to DTA-TGA for the different mixtures $ca_xdo_y^T$ based on calcite or / and dolomite

$(ca_xdo_y)^T$	Temperature of treatment (°C)	Mass loss (%)		
		30-200 (°C)	400-600 (°C)	600-800(°C)
$ca_{0.1}$	25	1.2	3.9	4.2
	600	0.6	0.2	4.9
	750	0.5	0.2	1.6
$ca_{0.5}$	25	0.6	3.6	22.1
	600	0.4	0.2	22.0
	750	0.3	0.2	22.3
$do_{0.1}$	25	1.2	6.0	4.3
	600	0.6	0.4	5.4
	750	0.5	0.3	1.7
$do_{0.5}$	25	0.6	3.7	23.1
	600	0.5	0.3	24.1
	750	0.4	0.2	23.9
$ca_{0.13}do_{0.05}$	25	1.2	5.1	11.3
	750	0.6	0.3	6.9

Table 3: S_{BET} and D_{50} values of different mixtures $ca_xdo_y^T$ based on calcite or/ and dolomite calcined at 600 and 750 °C

Sample	S_{BET} (m^2/g)	D_{50} (µm)
$ca_{0.1}^{600}$	18	23
$ca_{0.5}^{600}$	10	3
$do_{0.1}^{600}$	20	18
$do_{0.5}^{600}$	10	5
$ca_{0.1}^{750}$	19	18
$ca_{0.5}^{750}$	10	5
$do_{0.1}^{750}$	19	22
$do_{0.5}^{750}$	17	18
$ca_{0.13}do_{0.05}^{750}$	19	17

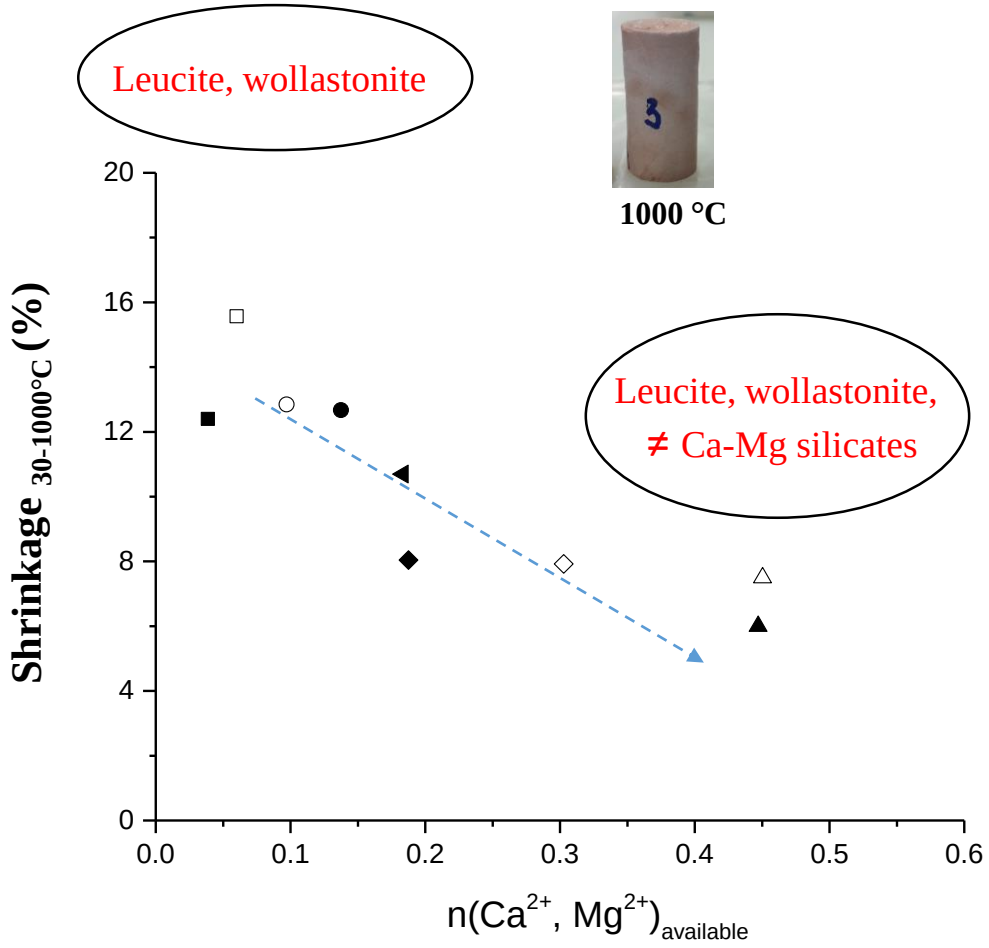

Kaolin-calcite and/or dolomite based geopolymers